Korean J Physiol Pharmacol
Vol 8: 33-41, February, 2004

Role of Stretch-Activated Channels in Stretch-Induced Changes of Electrical Activity in Rat Atrial Myocytes

Jae Boum Youm[1], Su-Hyun Jo[1], Chae Hun Leem[2], Won-Kyung Ho[3], and Yung E. Earm[3]

[1]Department of Physiology, Cheju National University College of Medicine, Jeju 690-756, [2]Department of Physiology and the Institute for Calcium Research, University of Ulsan College of Medicine, Seoul 138-736, [3]Department of Physiology and Biophysics, Seoul National University College of Medicine, Seoul 110-799, Korea

We developed a cardiac cell model to explain the phenomenon of mechano-electric feedback (MEF), based on the experimental data with rat atrial myocytes. It incorporated the activity of ion channels, pumps, exchangers, and changes of intracellular ion concentration. Changes in membrane excitability and Ca^{2+} transients could then be calculated. In the model, the major ion channels responsible for the stretch-induced changes in electrical activity were the stretch-activated channels (SACs). The relationship between the extent of stretch and activation of SACs was formulated based on the experimental findings. Then, the effects of mechanical stretch on the electrical activity were reproduced. The shape of the action potential (AP) was significantly changed by stretch in the model simulation. The duration was decreased at initial fast phase of repolarization (AP duration at 20% repolarization level from 3.7 to 2.5 ms) and increased at late slow phase of repolarization (AP duration at 90% repolarization level from 62 to 178 ms). The resting potential was depolarized from −75 to −61 mV. This mathematical model of SACs may quantitatively predict changes in cardiomyocytes by mechanical stretch.

Key Words: Stretch-activated channels, Mechanical stretch, Atrial myocyte

INTRODUCTION

It is well known that mechanical stress or dilation of the heart induces changes in electrical activity such as arrhythmias and altered diastolic membrane potential (Lab, 1978; Boland & Troquet, 1980; Dean & Lab, 1989; Franz et al, 1989; Hansen et al, 1990; Franz et al, 1992; Hansen, 1993). The changes in cardiac mechanical environment that leads to altered electrical activity are referred to as mechano-electric feedback (Lab, 1996; Kohl & Ravens, 2003). There is evidence that the major events of mechano-electric feedback are mediated by activation of SACs (Bustamante et al, 1991; Hagiwara et al, 1992; Sasaki et al, 1992; Craelius, 1993; Hoyer et al, 1994). It is, therefore, suggested that SACs may act as a mechano-transducer of mechano-electric feedback, which converts a mechanical stimulus into an electrical signal.

Using a rat atrial myocyte model, we demonstrated that direct stretch to atrial myocytes results in depolarization of the membrane potential (Zhang et al, 2000). Two microelectrodes were used to apply a mechanical stretch to a single atrial myocyte in a longitudinal direction, resulting in depolarization that was caused by activation of SACs with non-selectivity over cations. Recently, a cardiac model (Kyoto-Model) was developed to describe electrical activity, Ca^{2+} transients, and contractile force in guinea-pig sino-atrial node cells and ventricular myocytes (Matsuoka et al, 2003; Sarai et al, 2003). Ion channels, exchangers, and pumps were incorporated in the model to reproduce the electrical activity. Ca^{2+}-binding proteins and sarcoplasmic reticulum (SR) compartments were also incorporated to reproduce Ca^{2+} transients induced by the AP. Based on the Kyoto-Model and the experimental findings on the SACs in rat atrial myocytes, we developed a model to explain the effect of stretch on the electrical activity of heart. The shape of the AP and diastolic membrane potential was significantly changed by stretch in the model in agreement with previous and present experimental findings. The present model may provide a useful tool to understand the phenomenon of MEF.

Corresponding to: Yung E. Earm, Department of Physiology and Biophysics, Seoul National University College of Medicine, 28 Youngon-dong, Chongno-gu, Seoul 110-790, Korea. (Tel) +82-2-740-8224, (Fax) +82-2-763-9667, (E-mail) earmye@snu.ac.kr

METHODS

Cell preparation

Conforming to the Guide of the Committee for Animal Experiment of the College of Medicine, Seoul National University, Sprague-Dawley young adult rats (200~250 g) were killed by cervical dislocation. The hearts were isolated and perfused with 100 ml of oxygenated normal Tyrode solution (37°C). The perfusion solution was changed to 50 ml of nominally Ca^{2+}-free Tyrode solution, and then to the same solution containing 0.12 mg/ml collagenase (Yakult,

ABBREVIATIONS: SACs, stretch-activated channels; APD, action potential duration; MEF, mechano-electric feedback.

Japan) and 50 μM $CaCl_2$. After 14 min, the hearts were removed from the Langendorff apparatus and placed in a high-K^+, low-Cl^- storage medium. The atria and their appendages were dissected into small pieces and mechanically dispersed with a fire polished Pasteur pipette in the same solution. Isolated myocytes were stored in the high-K^+, low-Cl^- storage medium at 4°C until use.

Solutions

The high-K^+, low-Cl^- storage medium contained (in mM) 50 L-glutamate, 50 KCl, 20 taurine, 20 KH_2PO_4, 3 $MgCl_2$, 10 glucose, 10 HEPES (N-[2-hydroxyethyl]piperazine-N-[2-ethanesulfonic acid]), and 0.5 EGTA (ethyleneglycol-bis(β-aminoethyl ether)-*N,N,N',N'*-tetraacetic acid), and pH was adjusted to 7.3 with KOH. For the perfusion of myocytes in the electrophysiological recordings, normal Tyrode external solution and high K^+ (140 KCl) pipette solution were used. Normal Tyrode solution contained (in mM) 143 NaCl, 5.4 KCl, 0.5 $MgCl_2$, 1.8 $CaCl_2$, 5.5 glucose, and 5 HEPES (pH 7.4). External Cs^+ solutions contained (in mM) 140 CsCl, 2 $MgCl_2$, and 10 HEPES (pH 7.4). Internal Cs^+ solutions contained (in mM) 140 CsCl, 1 $MgCl_2$, 10 HEPES, 5 EGTA, 5 MgATP, 2.5 ditris-phosphocreatine, and 2.5 disodium phosphocreatine (pH 7.2). External or internal Na^+ solutions were prepared by replacing 140 mM CsCl with 140 mM NaCl. In hypotonic cell-inflation experiments, hypotonic and normotonic solutions were used. Hypotonic solutions (216 mOsm) contained (in mM) 100 CsCl, 2 $MgCl_2$, and 10 HEPES (pH 7.2). Normotonic solutions (296 mOsm) contained (in mM) 100 CsCl, 80 sucrose, 2 $MgCl_2$, and 10 HEPES. Unless otherwise noted, all chemicals were from Sigma (St. Louis, MO, USA).

Electrophysiological recordings

The standard whole-cell voltage clamp method (Hamill et al, 1981) was performed using an Axopatch-1C amplifier (Axon Instruments, CA, USA). Recording pipettes were fabricated and fire polished from 1.5 mm o.d. glass (Clark Electromedical, UK) to produce microelectrodes with resistances of 2~4 MΩ when filled with K^+-rich recording solution. A giga seal was made by applying negative pressure at approximately −10 mmHg, and seal resistance was usually above 2 GΩ. The current signals were filtered via a 1~10 kHz, 4-pole Bessel-type low-pass filter and digitized using Digidata 1200 (Axon Instruments) for subsequent analysis (pCLAMP software 6.0.1, Axon Instruments, CA, USA). In most experiments, the temperature was set at room temperature (20~24°C). All the data were averaged and normalized, and are presented as means±S.E.M. The reversal potentials were determined in each cell as the zero current intercept of the polynomial fit (4-order) to the current-voltage relationship.

Application of mechanical stretch

Mechanical stretch was applied by either hypo-osmotic cell inflation or direct stretch using two microelectrodes (Zhang et al, 2000). Hypo-osmotic cell inflation was achieved by changing the perfusion solution from the control normotonic solution (296 mOsm) to the hypotonic solution (216 mOsm). In order to identify hypo-osmotic stress, cells were placed in the hypotonic solution for ~3 minutes until a visible swelling occurred. The extent of direct stretch, using two microelectrodes, was expressed as the percentile change in cell length (L) relative to the original length:

$$(1)\quad \Delta L=(L_{stretch}-L_{original})/L_{original}\cdot 100$$

Mathematical model

The model of stretch-induced changes in electrical activity used in this study is based on the Kyoto-Model (Matsuoka et al, 2003; Sarai et al, 2003). This model can reproduce and describe the various cellular activities of cardiomyocytes such as AP, SR Ca^{2+} dynamics, and cell contraction. In order to reproduce them, the model incorporated ion channels, exchangers, pumps, Ca^{2+}-binding proteins, SR compartment, and contractile apparatus. The Kyoto-Model was originally developed to fit the experimental findings on the guinea-pig sino-atrial node cells and ventricular myocytes. We had to make some species-specific modification, because our experimental findings on the stretch-induced electrical activity are mainly from rat atrial myocytes (see Appendix). In order to create stretch-induced effects using this model, we also introduced the stretch-activated non-selective cation channels (SACs) and background non-selective cation channels.

Stretch-activated non-selective cation channels (SACs) in the model

The amplitude of I_{SAC} in rat atrial myocytes can be determined by the following equation with slight modification from the previous model (Sachs, 1994):

$$(2)\quad I_{SAC}/I_{SAC,\ max}=1/(1+\exp((\Delta L-\Delta L_{1/2})/(-s)))$$

I_{SAC} is defined as the current density (pA/pF) at each degree of direct stretch, $I_{SAC,\ max}$ the current density at maximum stretch without cell death or breakdown of the seal, and ΔL as the percentile change in cell length, which was already described in equation (1). $\Delta L_{1/2}$ is the ΔL where the I_{SAC} reaches half the amplitude of $I_{SAC,\ max}$. The s represents the slope factor describing the stretch sensitivity. Fitting the I_{SAC}−stretch relationship in our previous study (Zhang et al, 2000) to the equation (2) gives the value of 16.9% and 6.3%, corresponding to $\Delta L_{1/2}$ and s, respectively. Since $I_{SAC,\ max}$ shows a linear voltage dependence (Zhang et al, 2000), the amplitude can be expressed simply as the function of permeability and constant field equations (see Appendix) for each ion species without considering the voltage-dependent gating of channels. From the reversal potential (V_{rev}=−6.1 mV) in physiological salt solution, the permeability ratio of P_{Na}/P_K was calculated to be 0.76. The permeability ratio was then used in the model to calculate fluxes of each cation by activation of I_{SAC}.

Background non-selective cation channels in the model

Under the whole-cell voltage clamp, replacement of Na^+ with $NMDG^+$ significantly reduced the membrane conductance in rat atrial myocytes (Youm et al, 2000). This conductance still remained after blocking the time- and voltage-dependent ion channels under isotonic Na^+ condition.

Although non-selective over the cations, the permeability ratio (P_{Cs} : P_{Na} : P_{Li}=1.49 : 1 : 0.70) was different from that (P_{Cs} : P_{Na} : P_{Li}=1.05 : 1 : 0.98) of I_{SAC} (Zhang et al, 2000). This conductance was described in the model as the sum of cation components by their relative permeability ratios.

RESULTS

Reconstruction of whole-cell membrane currents

Employing the Kyoto-Model, we were able to reconstruct the whole-cell membrane currents of rat atrial myocytes with some modification to fit our experimental findings (see Appendix). In order to check the validity of our model, we measured the whole-cell membrane currents elicited by varying voltage steps between −120 and +100 mV (Fig. 1A, *left panel*), and compared them with the recordings by model simulation (Fig. 1B, *left panel*). In response to hyperpolarizing voltage steps, large inward currents appeared. The current jumps are mainly due to inward rectifier K^+ channel conductance. In response to depolarizing voltage steps, inward rectifier K^+ channel conductance still appeared, but with much smaller amplitude, showing the inward rectification. From −60 mV, a rapid and transient inward current was also noted, which is mainly due to activation of voltage gated Na^+ channel. From −20 mV, time- dependent outward current developed as a major conductance. This conductance is mainly due to activation of depolarization-activated outward K^+ channel. The depolarization-activated outward K^+ current is the main repolarization-inducing current in rat atrial myocytes (Boyle & Nerbonne, 1992). The current-voltage (*I-V*) relationship was obtained by applying voltage ramps (Fig. 1, *right and left panel*). The *I-V* relationship showed strong inward rectification, which is characteristic of cardiomyocytes. At the positive potential range, outward rectification was also evident. The reversal potential ranged between −75 and −65 mV.

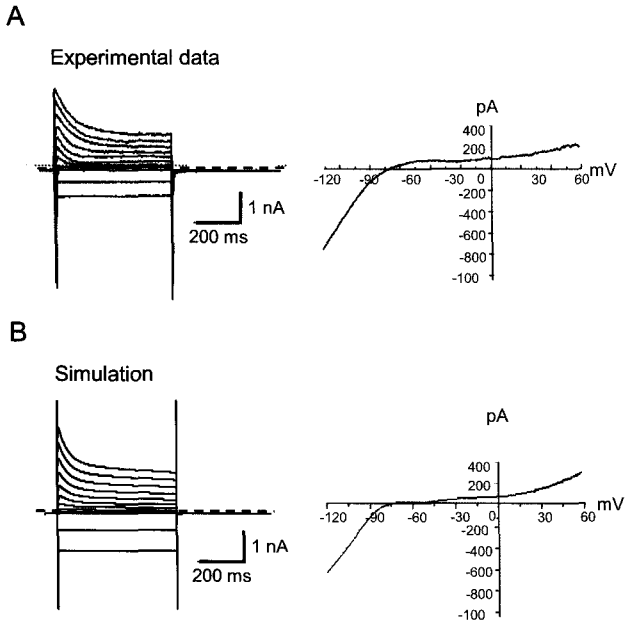

Fig. 1. Comparison of voltage clamp recordings in single rat atrial myocyte with those in model simulation. A, experimental recordings on voltage steps to −120~+100 mV from the holding potential of −80 mV (left panel) and I-V relationship (right panel) between −120 and +60 mV. The duration of voltage steps is 500 ms and the interval is 10 s. In order to obtain the I-V relationship, ramp pulses from −120 to +60 mV with dV/dt of −225 mV/s were applied to the cell every 15 s. The holding potential between ramp pulses was −30 mV. B, current recordings on voltage steps and I-V relationship by the model simulation.

Changes in I-V relationship induced by direct stretch or hypo-osmotic cell inflation

Mechanical stimuli that have been used at the single cell level include osmotic swelling, positive inflation pressure, mechanical indentation, and uniaxial mechanical stretch (Cazorla et al, 1999; Riemer & Tung, 2003). Since uniaxial mechanical stretch is generally assumed to be the most appropriate analogous to the stretch of tissue (Brady, 1991), we used it to study the effects of stretch on the *I-V*

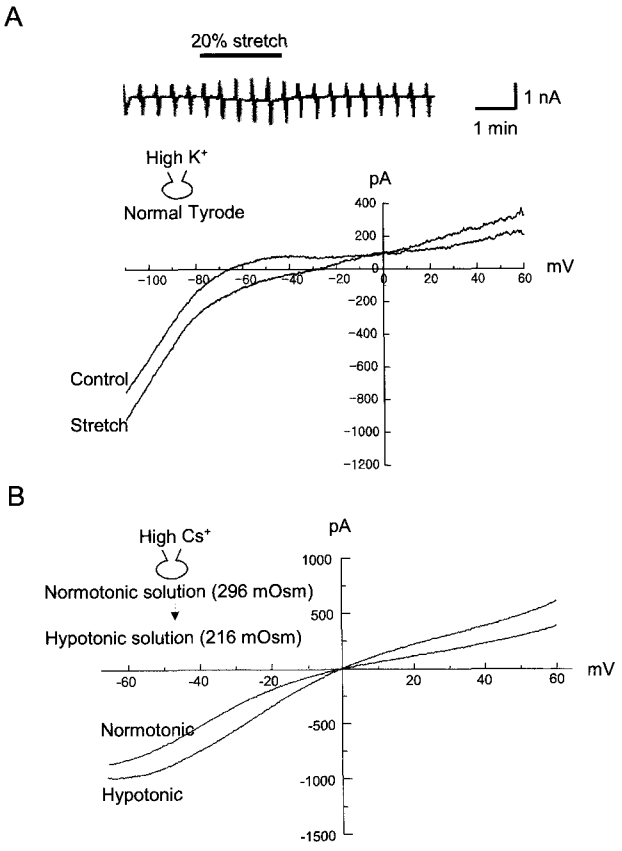

Fig. 2. Experimental recordings showing the effect of stretch on the I-V relationship. A, the effect of direct stretch by two microelectrodes on the I-V relationship. The same pulse protocol in Fig. 1B was used. Left upper inset shows the chart recording of current traces before, during, and recovery of stretch (20%) in normal Tyrode external and high K^+ internal solution. Lower inset shows the I-V relationship obtained from the left upper inset before and during stretch. B, the effect of hypo-osmotic cell inflation on the I-V relationship. Cells were inflated by changing the perfusion solution from normotonic to hypotonic Cs^+ solution (see Methods for details).

relationship. As shown in Fig. 2A, mechanical stretch increased inward and outward currents, and shifted the reversal potential into the positive direction. The reversal potential of stretch-induced current was around -6.1 ± 3.7 mV (n=7). We regarded the stretch-induced current as I_{SAC}. P_{Na}/P_K was calculated to be 0.76 by the reversal potential under physiological ion concentration. As an alternative way to induce membrane deformation, hypo-osmotic cell inflation has also been used (Ubl et al, 1988). Although hypotonic cell swelling or inflation causes stretch of cell membrane, it also causes a change in cell volume, resulting in activation of swelling-activated Cl^- current ($I_{Cl,swell}$) (Tseng 1992; Sakai et al, 1995; Li et al, 1996). As shown in Fig. 2B, perfusion of hypotonic solution for less than 3 min caused a linear increase of membrane currents. Since outward rectifying $I_{Cl,swell}$ is usually increased after 5 min, we regard the linear increase of membrane currents as SACs.

A model simulation of stretch was performed with the quantitative data such as permeability ratio, voltage dependence, and stretch dependence obtained from the above experimental findings, and Fig. 3 illustrates the stretch-induced changes in current traces and *I-V* relationship by the model simulation.

Stretch-induced changes in action potential (AP)

Uniaxial stretch of the single cardiomyocytes has been shown to decrease (Tung & Zou, 1995; White et al, 1993) or increase (Zeng et al, 2000) the action potential duration (APD). We tried to reproduce the effects of stretch on the AP by the model simulation based on the experimental findings from voltage-clamp study (Fig. 4B). As the conductance of SACs was increased, diastolic membrane potential was depolarized as a function of the degree of stretch (from -75 to -61 mV by 10% stretch). APD was also changed by varying degree of stretch: APD at 90% repolarization level was increased from 62 to 178 ms by 10% stretch, while it was decreased from 3.7 to 2.5 ms at 20% repolarization level, in good agreement with our previous data (Zhang et al, 2000), where direct stretch increased the APD and depolarized the diastolic membrane (Fig. 4A).

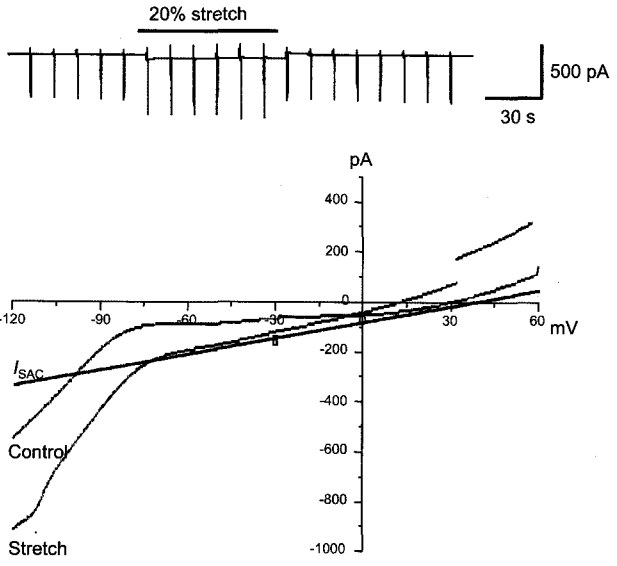

Fig. 3. The simulation recordings of current traces and I-V relationship before and during stretch. Pulse protocols and ionic concentrations are the same as those in Fig. 2A. The amplitude of I_{SAC} was determined by the equation (2) (see Methods for details).

Effects of ion permeability of SACs on the stretch-induced changes in AP

Activation of SACs leads to an increase in Ca^{2+} permeability. Since the SACs are permeable to Na^+, it is expected that activation of the SACs also increases Na^+ permeability. We, therefore, felt it important to evaluate which one was more crucial in the stretch-induced changes of the AP, and tested this by reducing the permeability of each ion through SACs. As shown in Fig. 5B, reducing Ca^{2+} permeability to 0 had no effect on the stretch-induced changes of the AP, however, reducing Na^+ permeability abolished the stretch-induced AP changes (Fig. 5C).

Model predictions of Ca^{2+} transients during stretch

Fig. 6 shows the model-predicted effects of stretch on the Ca^{2+} transients. Ten% stretch increased the amplitude and duration of Ca^{2+} transients without a significant change in the diastolic $[Ca^{2+}]_i$ (Fig. 6A). The amplitude of Ca^{2+} transients was gradually increased by stretch, implying a

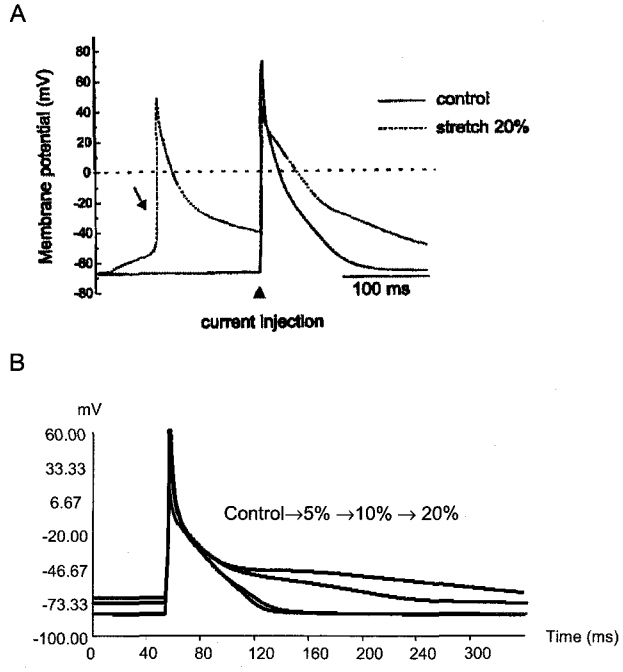

Fig. 4. Comparison of the effects of direct stretch on the membrane potentials by experimental findings with those by the model simulation. A, the effects of direct stretch (20%) on the diastolic membrane potential and AP. The diastolic membrane was depolarized by stretch. The duration of AP was increased by stretch. From the permission of Zhang et al (2000). B, the model simulation of direct stretch by 5%, 10%, and 20%. The model simulation also depolarized the diastolic membrane and increased the duration of AP stretch-dependently.

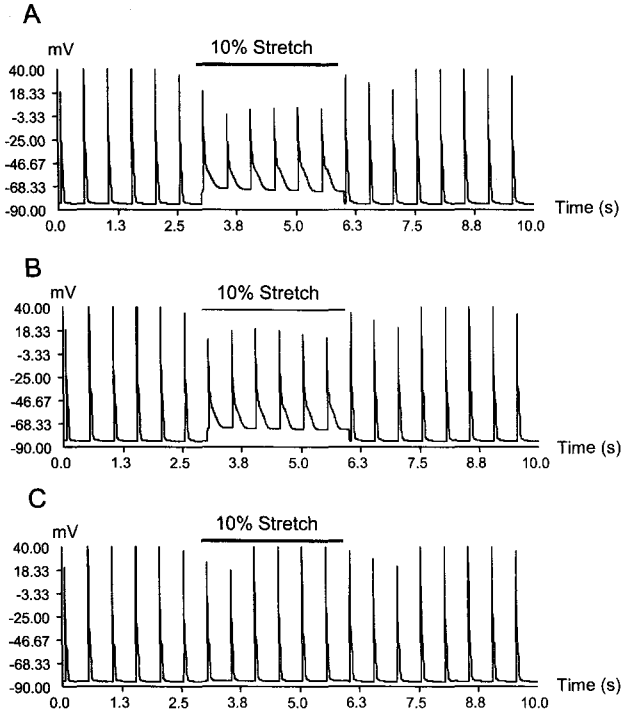

Fig. 5. The model predictions of AP changes by SACs with different ionic permeability. A, control prediction of the APs, when $P_K : P_{Na} : P_{Ca}$ through SACs is 1 : 0.76 : 0.70. B, prediction of the APs, when P_{Ca} is 0. Reducing the Ca^{2+} permeability through SACs did not affect the changes in shape of the APs by stretch. C, prediction of the APs, when P_{Na} is 0. Reducing the Na^+ permeability through SACs nearly abolished the effects of stretch on the APs.

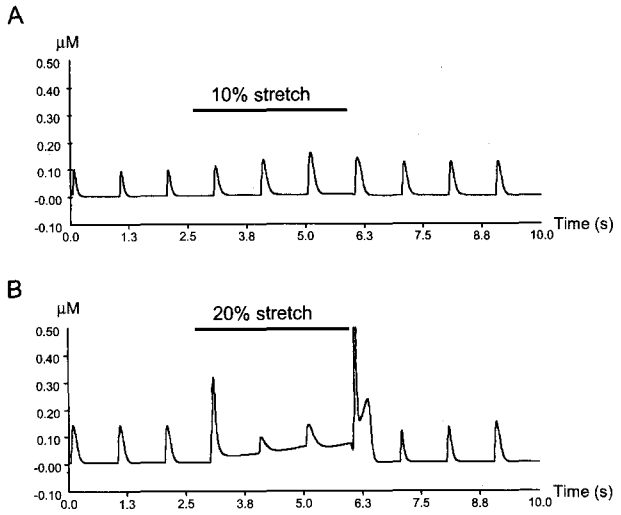

Fig. 6. The model predictions of the Ca^{2+} transients by different degree of stretch. A, changes in Ca^{2+} transients by 10% stretch. Stimulus interval is 1 s. B, changes in Ca^{2+} transients by 20% stretch.

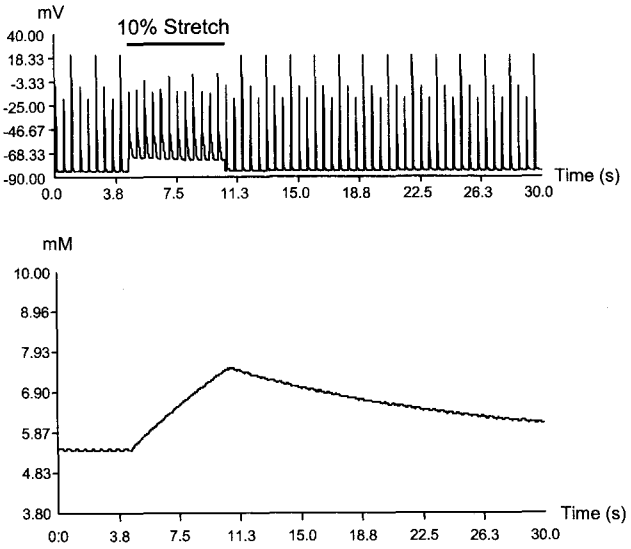

Fig. 7. The model predictions of the $[Na^+]_i$ during sustained stretch. $[Na^+]_i$ was gradually increased by sustained stretch and decreased very slowly by release of stretch (lower panel). Accompanying APs were also shown (upper panel). Stimulus interval is 0.5 s.

cumulative effect of sustained stretch. Twenty% stretch, however, gradually increased the diastolic $[Ca^{2+}]_i$ rather than the amplitude of Ca^{2+} transients (Fig. 6B).

Model predictions of $[Na^+]_i$, Na^+/K^+ pump, and Na^+/Ca^{2+} exchanger during stretch

Since the SACs are permeable to Na^+, their activation should increase $[Na^+]_i$. In the model, sustained stretch gradually increased $[Na^+]_i$ (Fig. 7, *lower panel*), and release of stretch decreased $[Na^+]_i$ very slowly. Accumulation of $[Na^+]_i$ has been shown to increase the outward current via the Na^+/K^+ pump. The model simulation clearly demonstrates the increase of outward current by activation of the Na^+/K^+ pump (Fig. 8A). Activation of the Na^+/K^+ pump may reduce the depolarizing effect of stretch. Fig. 8B shows the model simulation of Na^+/Ca^{2+} exchanger current during stretch. The amplitude of the current was decreased in the early phase of the AP, but increased in the later phase, suggesting a significant increase in Ca^{2+} influx in the later phase of the AP during stretch.

DISCUSSION

The objective of the present study was to reconstruct the stretch-induced changes of electrical activity in rat atrial myocytes, based on the experimental findings. The experimental part of the study demonstrates that mechanical stretch increases the membrane currents and shifts the reversal potential into the positive direction. The increase of membrane currents is mainly due to the increased conductance of the SACs. The modeling part of the study demonstrates that introducing the SACs can produce stretch-induced changes in AP. Both the modeling and experimental studies show that stretch of the single atrial myocytes depolarizes and prolongs the AP. The model suggests that the increased Ca^{2+} permeability through SACs does not have a significant effect on the changes in

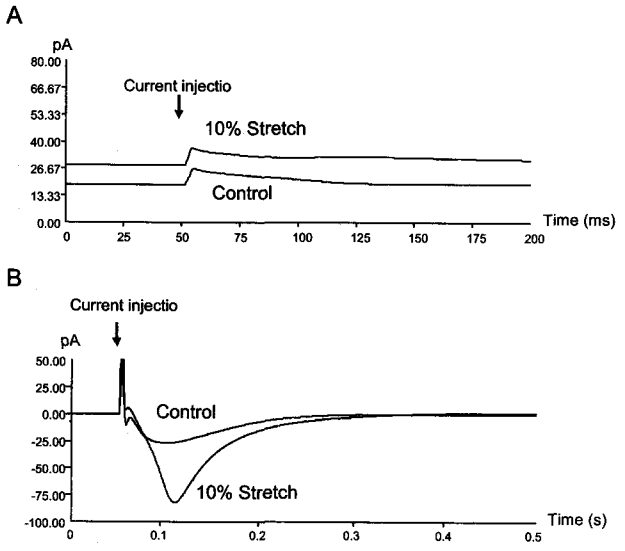

Fig. 8. The model predictions of I_{NaK} and I_{NaCa} during stretch. A, current traces of Na^+/K^+ pump before and after sustained stretch (8 s). The extent of stretch was 10%. B, current traces of Na^+/Ca^{2+} exchanger during AP before and after sustained stretch (8 s).

AP during stretch. Instead, the increased Na^+ permeability and delayed increase of the Na^+/Ca^{2+} exchanger current are likely to prolong and depolarize the AP. The model also suggests that a moderate stretch (10%) prolongs the AP without effect on the diastolic $[Ca^{2+}]_i$, while a severe stretch (20%) gradually increases the diastolic $[Ca^{2+}]_i$ in addition to the effect of AP prolongation. Finally, sustained stretch is suggested to increase $[Na^+]_i$ by increased Na^+ permeability in the model.

Role of the SACs

I_{SAC} induced by mechanical stretch in rat atrial myocytes showed a nearly linear voltage dependence and reversed polarity near −6 mV under physiological ionic conditions. I_{SAC} has also been analyzed with similar technique in human (Kamkin et al, 2000), guinea-pig (Sasaki et al, 1992; Kamkin et al, 2000; Calaghan et al, 2003), rat (Kamkin et al, 2000), mouse (Kamkin et al, 2003), and frog (Riemer & Tung, 2003) ventricular cells. In most cases, I_{SAC} showed voltage dependence and reversal potential similar to our results. Since the reversal potential of the I_{SAC} is near 0 mV, I_{SAC} is thought to act as outward currents at positive potentials and inward currents at negative potentials. Therefore, activation of the I_{SAC} can speed up early repolarization and retard late repolarization. In addition, activation of the I_{SAC} should depolarize the diastolic cell membrane, because stretch shifts the currents to more negative values at negative potentials. In agreement with this, activation of the I_{SAC} in the model simulation caused a decrease in APD at positive potentials and an increase in APD at negative potentials, thus the two APs crossing over (Fig. 4B). Mechanical stretch also induced depolarization of the diastolic membrane in the model simulation. In guinea-pig ventricular myocytes, direct mechanical stretch induced the diastolic depolarization and AP prolongation (Kamkin et al, 2000). Calaghan et al (2003) also found that direct mechanical stretch of guinea-pig ventricular myocytes prolongs the AP, however, it is not easy to explain why there is a great difference in APD between 5% and 10% stretch (at 90% repolarization level 70 and 178 ms, respectively). Activation of I_{SAC} alone is not sufficient to explain such a prominent difference in AP prolongation, because activation of the I_{SAC} is not quite different between them ($I_{SAC}/I_{SAC,max}$ 0.13 and 0.25, respectively). Tavi et al (1998) suggested that SACs do not directly modulate the APs, but the effects are mediated rather by the SR through the increased Ca^{2+} release during systole. They also suggested that the increased Na^+/Ca^{2+} exchanger inward current by increased Ca^{2+} release would directly modulate APs. Although the exact mechanism is not yet clear, it is thought that the small increase in APD and diastolic depolarization by moderate stretch is mainly due to activation of the I_{SACs}, while the prominent increase in APD by severe stretch is linked to the additional events mediated by increased Ca^{2+} transients. If Ca^{2+} transient mediates the prominent increase in APD during stretch, discussion on the major pathway of Ca^{2+} influx is in order. The majority of SACs has considerable permeability to both monovalent and divalent cations (Sachs, 1988), therefore, activation of the SACs should lead to an increase in $[Ca^{2+}]_i$. However, our model demonstrates that Ca^{2+} influx through SACs does not have a role in AP prolongation during stretch (Fig. 5). When Na^+ and Ca^{2+} were assumed to have an equal permeability through SACs under physiological ion concentration, Na^+ flux was 42 times larger than Ca^{2+} flux in the model calculation, thus explaining the reason why Ca^{2+} influx through SACs does not have a significant role in AP prolongation during stretch. In the cardiac cell, the major Ca^{2+} influx pathway is the L-type Ca^{2+} current ($I_{Ca,L}$). Axial stretch caused no increase in $I_{Ca,L}$ in guinea-pig, ferret, or rat myocytes (Sasaki et al, 1992; Hongo et al, 1996; Kamkin et al, 2000; Belus & White, 2003). However, there is a possibility that extra Ca^{2+} might enter the cell via $I_{Ca,L}$ due to delayed voltage-dependent inactivation during the lengthened depolarization (Calaghan et al, 2003). Further investigation is in need to make it clear which one is the major pathway of Ca^{2+} influx during stretch.

$[Ca^{2+}]_i$ change during stretch

Stretch of intact heart, isolated muscle, and the single myocyte causes immediate increase in force, followed by a secondary, slower increase in force that takes place over several minutes (Parmley & Chuck, 1973; Tucci et al, 1984; White et al, 1995). Allen and Kurihara (1982) showed that the slow response is associated with a corresponding increase in the magnitude of the Ca^{2+} transients. Our model clearly demonstrates the increase in the amplitude of the Ca^{2+} transients during moderate stretch (Fig. 6A). The results on the change of the diastolic $[Ca^{2+}]_i$ are controversial. There are some studies to show the increase in diastolic $[Ca^{2+}]_i$ (White et al, 1993; Gannier et al, 1994; Gannier et al, 1996), while conflicting studies to show no change of diastolic $[Ca^{2+}]_i$ during stretch (Hongo et al, 1996; Tavi et al, 1998). Our model simulation suggests that the severe sustained stretch (20%) can produce a gradual increase in the diastolic $[Ca^{2+}]_i$ (Fig. 6B). It is highly likely that a moderate increase of Ca^{2+} influx is well counterbalanced by Na^+/Ca^{2+} exchanger or plasmalemma Ca^{2+} pump, however, a severe increase in Ca^{2+} influx eventually leads to Ca^{2+} accumulation.

$[Na^{2+}]_i$ change during stretch

Since the SACs is permeable to Na^+, sustained stretch is expected to increase $[Na^+]_i$. There is evidence to show that stretch increased the cytosolic and total Na^+ concentration in human, mouse, and rat ventricular myocytes (Isenberg et al, 2003). Na^+ accumulation leads to an increased activity of Na^+/K^+ pump. Our model simulation shows the changes in $[Na^+]_i$ (Fig. 7) and activity of Na^+/K^+ pump (Fig. 8A) during sustained stretch. Increased Na^+/K^+ pump activity may augment the fast repolarization at positive potentials during stretch and serve as a counter-current mechanism that stabilizes the membrane potential during diastole.

APPENDIX

The mathematical model of the rat atrial myocytes

The mathematical model we used in this study is a modification of the Kyoto-Model (Matsuoka et al, 2003; Sarai et al, 2003) to fit the experimental findings on rat atrial myocytes. The model has been built with Visual C++ software in a window-based computer. A full description of the model is beyond the scope of this paper. However, it should be noted that some modifications of the Kyoto-Model were made. The integration algorithms were further developed to reduce errors in calculation. Ionic currents through the inward rectifier K^+ channel (I_{K1}) and depolarization-activated outward K^+ channel ($I_{K,out}$) were modified to fit the experimental results of our voltage clamp study in rat atrial myocytes. The volume of cell and compartments of SR were all adjusted to those of the rat atrial myocytes. Ionic concentrations were also modified to be the same as those used in our experimental work.

Integration algorithms

The numerical integration is based on the Runge-Kutta method described in the Kyoto-Model. For the two-state gating model, an alternative approach was used to reduce an excessive error in calculation by Runge-Kutta method.

In general, the following mono-exponential function is the general solution to the gating of two-state model

(3) $y(t)=a+b \cdot \exp(-t/\tau)$

where t is the time variable, τ is the time constant, and y(t) is the probability of the gate being in the permissive state at time t. The time constant is determined as the reciprocal of the sum of forward and backward rate constants.

The gating at time t_0 can thus be written as

(4) $y(t_0)=a+b \cdot \exp(-t_0/\tau)$

The gating after a time step Δt can be written as

(5) $y(t_0+\Delta t)=a+b \cdot \exp(-(t_0+\Delta t)/\tau)$

The first-order differential equation of $y(t_0)$ can be written as

(6) $dy(t_0)/dt=-b/\tau \cdot \exp(-t_0/\tau)$

Combining equations (4) and (6) gives the following two equations for a and b in terms of the variables at time t_0 and time constant (τ).

(7) $a=y(t_0)+\tau \cdot dy(t_0)/dt$

(8) $b=-\tau \cdot dy(t_0)/dt/\exp(-t_0/\tau)$

Now, we can get the value of $y(t_0+\Delta t)$ after a time step Δt by replacing a and b in equation (5) by the terms on the right side of the above equation (7) and (8), respectively.

(9) $y(t_0+\Delta t)=y(t_0)+\tau \cdot dy(t_0)/dt-\tau \cdot dy(t_0)/dt/\exp(-t_0/\tau) \cdot \exp(-(t_0+\Delta t)/\tau)$

The term on the left side of the following equation (10) equals the term on the right side.

(10) $\exp(-(t_0+\Delta t)/\tau)=\exp(-t_0/\tau) \cdot \exp(-\Delta t/\tau)$

Combining eqaution (9) and (10) gives the following equation.

(11) $y(t_0+\Delta t)=y(t_0)+\tau \cdot dy(t_0)/dt \cdot (1-\exp(-\Delta t/\tau))$

Then, we can use equation (11) to get $y(t_0+\Delta t)$ in terms of the variables $y(t_0)$ and $dy(t_0)/dt$ at time t_0.

Model formulations for the inward rectifier K^+ current (I_{K1})

$$C \underset{\beta_n}{\overset{\alpha_n}{\rightleftarrows}} O$$

State O goes into state B reversibly,

$$O \underset{\lambda}{\overset{\mu}{\rightleftarrows}} B$$

(12) $I_{K1}=G_{IK1} \cdot (V-E_K) \cdot n \cdot f_U$

(13) $E_K=-86.7([K^+]_i=140\ mM,\ [K^+]_o=5.4\ mM)$

(14) $\alpha_n=1.0/(8000 \cdot \exp((V-E_K-97)/8.5)+7 \cdot \exp((V-E_K-97)/300))$

(15) $\beta_n=1.0/(0.00014 \cdot \exp((V-E_K-97)/(-9.1))+0.2 \cdot \exp((V-E_K-97)/(-500)))$

(16) $\mu=12.75 \cdot \exp(0.035 \cdot (V-E_K-10))/(1+\exp(0.015 \cdot (V-E_K-140)))$

(17) $\lambda=3 \cdot \exp(-0.048 \cdot (V-E_K-10)) \cdot (1+\exp(0.064 \cdot (V-E_K-38)))/(1+\exp(0.03 \cdot (V-E_K-70)))$

(18) $f_B=\mu/(\mu+\lambda)$

(19) $f_U=\lambda/(\mu+\lambda)$

Model formulations for the depolarization-activated outward K^+ current ($I_{K,out}$)

(20) $I_{K,out}=I_{K,fast}+I_{K,slow}$

(21) $I_{K,fast}=I_{K,fast}K+I_{K,fast}Na$

(22) $I_{K,fast}K=2.9 \cdot m \cdot h \cdot K_{CF}$

(23) $I_{K,fast}Na=0.26 \cdot m \cdot h \cdot Na_{CF}$

(24) $\alpha_m(I_{K,fast})=1/(1.4 \cdot \exp(V/(-14241))+0.35 \cdot \exp(V/(-15)))$

(25) $\beta_m(I_{K,fast})=1/(22.7 \cdot \exp(V/37.9)+1775 \cdot \exp(V/8.4))$

(26) $\alpha_h(I_{K,fast})=1/(2.5 \cdot \exp(V/3.2)+2195 \cdot \exp(V/23.6))$

(27) $\beta_h(I_{K,fast})=1/(40.4 \cdot \exp(V/(-76022))+0.29 \cdot \exp(V/(-5.4)))$

(28) $I_{K,slow}=I_{K,slow}K+I_{K,slow}Na$

(29) $I_{K,slow}K=1.8 \cdot m \cdot h \cdot K_{CF}$

(30) $I_{K,slow}Na=0.16 \cdot m \cdot h \cdot Na_{CF}$

(31) $\alpha_m(I_{K,slow})=1/(0.0002 \cdot \exp(V/(-7.2))+1.37 \cdot \exp(V/(-47.8)))$

(32) $\beta_m(I_{K,slow})=1/(1346 \cdot \exp(V/16.0)+1600 \cdot \exp(V/11.3))$

(33) $\alpha_h(I_{K,slow})=1/(6613 \cdot \exp(V/135222)+143392 \cdot \exp(V/12.1))$

(34) $\beta_h(I_{K,slow})=1/(4801 \cdot \exp(V/(-125))+119 \cdot \exp(V/(-10.3)))$

Constant field equations

(35) $$K_{CF}=\frac{F \cdot V}{R \cdot T} \frac{[K^+]_i-[K^+]_o \cdot \exp\left(\frac{-F \cdot V}{R \cdot T}\right)}{1-\exp\left(\frac{-F \cdot V}{R \cdot T}\right)}$$

(36) $$Na_{CF}=\frac{F \cdot V}{R \cdot T} \frac{[Na^+]_i-[Na^+]_o \cdot \exp\left(\frac{-F \cdot V}{R \cdot T}\right)}{1-\exp\left(\frac{-F \cdot V}{R \cdot T}\right)}$$

(37) $$Ca_{CF}=\frac{2 \cdot F \cdot V}{R \cdot T} \frac{[Ca^{2+}]_i-[Ca^{2+}]_o \cdot \exp\left(\frac{-2 \cdot F \cdot V}{R \cdot T}\right)}{1-\exp\left(\frac{-2 \cdot F \cdot V}{R \cdot T}\right)}$$

Initiall parameters

Cell volume (μm^3): $V_i=4046\,\mu m^3$
SR release site (μm^3): $V_{rel}=0.02 \times V_i$
SR uptake site (μm^3): $V_{up}=0.05 \times V_i$
Membrane capacitance (pF): $C_m=50$
Cytosolic $[K^+]$ (mM): $[K^+]_i=140$
Cytosolic $[Na^+]$ (mM): $[Na^+]_i=5.4$
Cytosolic $[Ca^{2+}]$ (μM): $[Ca^{2+}]_i=0.0035$
Extracellular $[K^+]$ (mM): $[K^+]_o=5.4$
Extracellular $[Na^+]$ (mM): $[Na^+]_o=140$
Extracellular $[Ca^+]$ (mM): $[Ca^{2+}]_o=1.8$
Access resistance of microelectrode ($M\Omega$): $R_a=2.5$
Temperature (°C): T=36

Definition of symbols

I_{K1}: inward rectifier K^+ current
$I_{K,out}$: depolarization-activated outward K^+ current
$I_{K,fast}$: fast component of depolarization-activated outward K^+ current
$I_{K,slow}$: slow component of depolarization-activated outward K^+ current
m, h: activation and inactivation gate of $I_{K,out}$, respectively
n: activation gate of I_{K1}
f_B: fraction of block
f_U: fraction of unblock
α_n and β_n: opening and closing rate constants, respectively, of I_{K1}, ms^{-1}
μ: rate constant of block, of I_{K1}, ms^{-1}
λ: rate constant of unblock, of I_{K1}, ms^{-1}
α_m and β_m: opening and closing rate constants, respectively, of activation gate, ms^{-1}
α_h and β_h: opening and closing rate constants, respectively, of inactivation gate, ms^{-1}
V: membrane potential, mV
E_K: reversal potential of K^+, mV

ACKNOWLEDGEMENTS

This work was supported in part by funds from Advanced Backbone IT Technology Development Project of Ministry of Information and Communication (IMT-2000-C3-5), and a Non Directed Research Fund from the Korea Research Foundation (1996). We thank Drs. A. Noma, N. Sarai, S. Matsuoka for introducing Kyoto-Model to us.

REFERENCES

Allen DG, Kurihara S. The effects of muscle length on intracellular calcium transients in mammalian cardiac muscle. *J Physiol* 327: 79-94, 1982

Belus A, White E. Streptomycin and intracellular calcium modulate the response of single guinea-pig ventricular myocytes to axial stretch. *J Physiol* 546: 501-509, 2003

Boland J, Troquet J. Intracellular action potential changes induced in both ventricles of the rat by an acute right ventricular pressure overload. *Cardiovasc Res* 14: 735-740, 1980

Boyle WA, Nerbonne JM. Two functionally distinct 4-aminopyridine-sensitive outward K^+ currents in rat atrial myocytes. *J Gen Physiol* 100: 1041-1067, 1992

Brady AJ. Mechanical properties of isolated cardiac myocytes. *Physiol Rev* 71: 413-428, 1991

Bustamante JO, Ruknudin A, Sachs F. Stretch-activated channels in heart cells: relevance to cardiac hypertrophy. *J Cardiovasc Pharmacol* 17: S110-S113, 1991

Calaghan SC, Belus A, White E. Do stretch-induced changes in intracellular calcium modify the electrical activity of cardiac muscle? *Prog Biophys Mol Biol* 82: 81-95, 2003

Cazorla O, Pascarel C, Brette F, Le Guennec JY. Modulation of ions channels and membrane receptors activities by mechanical interventions in cardiomyocytes: possible mechanisms for mechanosensitivity. *Prog Biophys Mol Biol* 71: 29-58, 1999

Craelius W. Stretch-activation of rat cardiac myocytes. *Exp Physiol* 78: 411-423, 1993

Dean JW, Lab MJ. Arrhythmia in heart failure: role of mechanically induced changes in electrophysiology. *Lancet* 1: 1309-1312, 1989

Franz MR, Burkhoff D, Yue DT, Sagawa K. Mechanically induced action potential changes and arrhythmia in isolated and in situ canine hearts. *Cardiovasc Res* 23: 213-223, 1989

Franz MR, Cima R, Wang D, Profitt D, Kurz R. Electrophysiological effects of myocardial stretch and mechanical determinants of stretch-activated arrhythmias. *Circulation* 86: 968-978, 1992 Erratum in: *Circulation* 86: 1663, 1992

Gannier F, White E, Garnier, Le Guennec JY. A possible mechanism for large stretch-induced increase in $[Ca^{2+}]_i$ in isolated guinea-pig ventricular myocytes. *Cardiovasc Res* 32: 158-167, 1996

Gannier F, White E, Lacampagne A, Garnier D, Le Guennec JY. Streptomycin reverses a large stretch induced increases in $[Ca^{2+}]_i$

in isolated guinea pig ventricular myocytes. *Cardiovasc Res* 28: 1193–1198, 1994

Hagiwara N, Irisawa H, Kasanuki H, Hosoda S. Background current in sino-atrial node cells of the rabbit heart. *J Physiol* 448: 53–72, 1992

Hansen DE. Mechanoelectrical feedback effects of altering preload, afterload, and ventricular shortening. *Am J Physiol* 264: H423–H432, 1993

Hansen DE, Craig CS, Hondeghem LM. Stretch-induced arrhythmias in the isolated canine ventricle. Evidence for the importance of mechanoelectrical feedback. *Circulation* 81: 1094–1105, 1990

Hongo K, White E, Le Guennec JY, Orchard CH. Changes in $[Ca^{2+}]_i$, $[Na^+]_i$ and Ca^{2+} current in isolated rat ventricular myocytes following an increase in cell length. *J Physiol* 491: 609–619, 1996

Hoyer J, Distler A, Haase W, Gogelein H. Ca^{2+} influx through stretch-activated cation channels activates maxi K^+ channels in porcine endocardial endothelium. *Proc Natl Acad Sci USA* 91: 2367–2371, 1994

Isenberg G, Borschke B, Rueckschloss U. Ca^{2+} transients of cardiomyocytes from senescent mice peak late and decay slowly. *Cell Calcium* 34: 271–280, 2003

Kamkin A, Kiseleva I, Isenberg G. Stretch-activated currents in ventricular myocytes: amplitude and arrhythmogenic effects increase with hypertrophy. *Cardiovasc Res* 48: 409-420, 2000

Kamkin A, Kiseleva I, Isenberg G. Ion selectivity of stretch-activated cation currents in mouse ventricular myocytes. *Pflugers Arch* 446: 220–231, 2003

Kohl P, Ravens U. Cardiac mechano-electric feedback: past, present, and prospect. *Prog Biophys Mol Biol* 82: 3–9, 2003

Lab MJ. Mechanically dependent changes in action potentials recorded from the intact frog ventricle. *Circ Res* 42: 519-528, 1978

Lab MJ. Mechanoelectric feedback (transduction) in heart: concepts and implications. *Cardiovasc Res* 32: 3–14, 1996

Li GR, Feng JL, Wang ZG, Nattel S. Transmembrane chloride currents in human atrial myocytes. *Am J Physiol* 270: C500–C507, 1996

Matsuoka S, Sarai N, Kuratomi S, Ono K, Noma A. Role of individual ionic current systems in ventricular cells hypothesized by a model study. *Jpn J Physiol* 53: 105–123, 2003

Parmley WW, Chuck L. Length-dependent changes in myocardial contractile state. *Am J Physiol* 224: 1195–1199, 1973

Riemer TL, Tung L. Stretch-induced excitation and action potential changes of single cardiac cells. *Prog Biophys Mol Biol* 82: 97–110, 2003

Sachs F. Mechanical transduction in biological systems. *Crit Rev Biomed Eng* 16: 141–169, 1988

Sakai R, Hagiwara N, Kasanuki H, Hosoda S. Chloride conductance in human atrial cells. *J Mol Cell Cardiol* 27: 2403-2408, 1995

Sarai N, Matsuoka S, Kuratomi S, Ono K, Noma A. Role of individual ionic current systems in the SA node hypothesized by a model study. *Jpn J Physiol* 53: 125–134, 2003

Sasaki N, Mitsuiye T, Noma A. Effects of mechanical stretch on membrane currents of single ventricular myocytes of guinea-pig heart. *Jpn J Physiol* 42: 957–970, 1992

Tavi P, Han C, Weckstrom M. Mechanisms of stretch-induced changes in $[Ca^{2+}]_i$ in rat atrial myocytes: role of increased troponin C affinity and stretch-activated ion channels. *Circ Res* 83: 1165–77, 1998

Tseng GN. Cell swelling increases membrane conductance of canine cardiac cells: evidence for a volume-sensitive Cl channel. *Am J Physiol* 262: C1056–1068, 1992

Tucci PFJ, Bregagnollo EA, Spadaro J, Cicogna AC, Ribeiro MCL. Length dependence of activation studied in the isovolumic blood-perfused dog heart. *Circ Res* 55: 59–66, 1984

Tung L, Zou S. Influence of stretch on excitation threshold of single frog ventricular cells. *Exp Physiol* 80: 221–235, 1995

Ubl J, Murer H, Kolb HA. Hypotonic shock evokes opening of Ca^{2+}-activated K channels in opossum kidney cells. *Pflugers Arch* 412: 551–553, 1988

White E, Le Guennec JY, Nigretto JM, Gannier F, Argibay JA, Garnier D. The effects of increasing cell length on auxotonic contractions; membrane potential and intracellular calcium transients in single guinea-pig ventricular myocytes. *Exp Physiol* 78: 65–78, 1993

Youm JB, Ho WK, Earm YE. Permeability characteristics of monovalent cations in atrial myocytes of the rat heart. *Exp Physiol* 85: 143–150, 2000

Zeng T, Bett GCL, Sachs F. Stretch-activated whole cell currents in adult rat cardiac myocytes. *Am J Physiol* 278: H548–H557, 2000

Zhang YH, Youm JB, Sung HK, Lee SH, Ryu SY, Ho WK, Earm YE. Stretch-activated and background non-selective cation channels in rat atrial myocytes. *J Physiol* 523: 607–619, 2000